Supplementary Information (SI) for Nanoscale.

Supporting Information

A Non-Enzymatic Dual Sensing Approach for the Detection of Cholesterol in Human Blood Serum, Rat Blood Serum, and Milk using Silk Fiber Functionalized Phosphorene Quantum Dots

Nasrin Sultana[1,2], Shreyash Vijay Andagonde[1], Ratul Chakraborty[1,2], Asis Bala[1,2], Neelotpal Sen Sarma[1,2*]

[1]Institute of Advanced Study in Science and Technology, Paschim Boragaon, Guwahati-35, Assam, India

[2]Academy of Scientific and Innovative Research (AcSIR), Ghaziabad-201002, India

***Corresponding author**: neelot@iasst.gov.in

Figure S1(a & b) shows the AFM images of the exfoliated Ph. We have analyzed the AFM images in the scale 1µm × 1µm and 400 nm × 400 nm. After recording the images, with the help of WSxM 5.0 we did the height profiling. In case of the 1µm × 1µm scale, the average height of the exfoliated sheets was found to be about 40.5 nm and for 400 nm × 400 nm the obtained average height was about 19.2 nm.

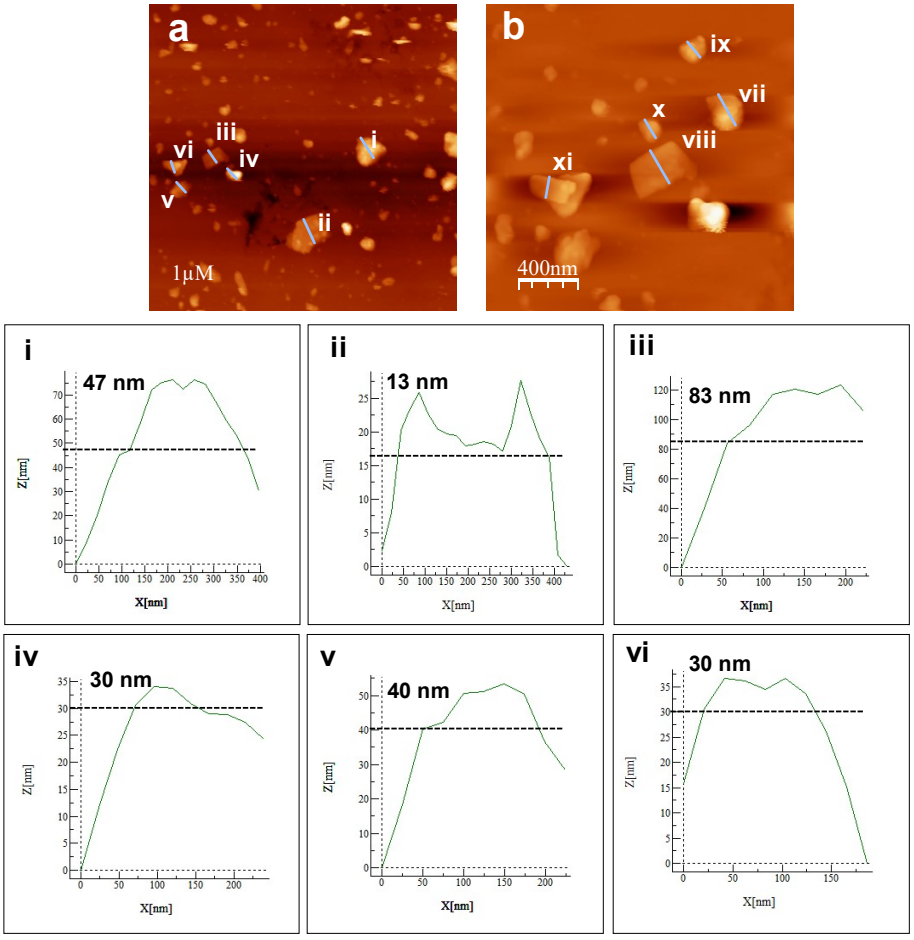

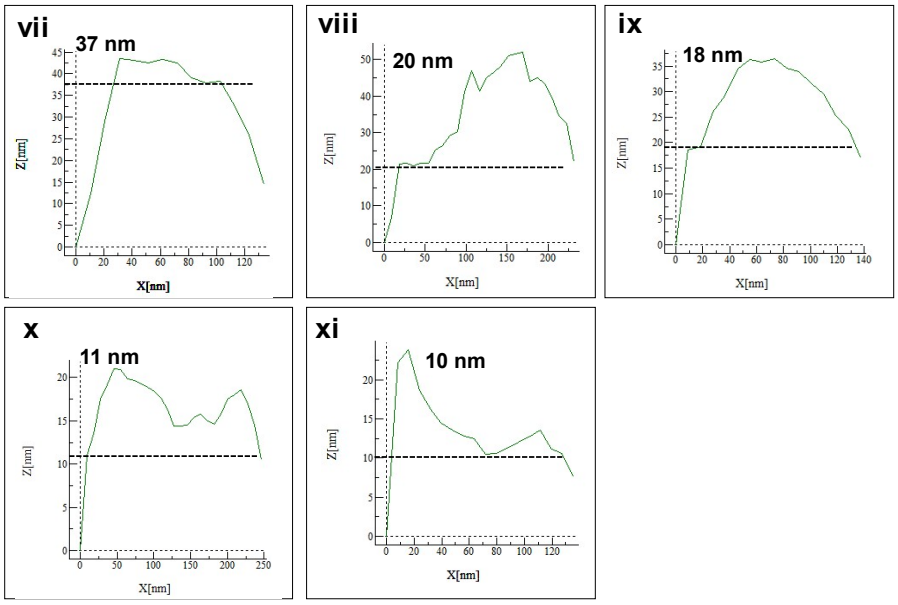

Figure S1. AFM images of exfoliated Ph in the scale 1µm × 1µm and 400 nm × 400 nm along with the height profiling i.e., (i-vi) for the scale 1µm × 1µm and (vii-xi) for the scale 400 nm × 400 nm

Figure S2 shows the excitation and emission spectra of the synthesized composite i.e., Ph-SF. Before carrying out the optical property analysis, we checked the optimum excitation wavelength where the emission wavelength was maximum. It has been observed that, upon exciting the material at 310 nm it shows a maximum emission wavelength of about 420 nm. We have excited the material in the range of 250- 360 nm to find out the maximum emission (*figure S2a*). Along with this, we have also recorded the excitation spectra at various emission wavelengths ranging from 350-460 nm to further confirm that the emission maxima are at 420 nm (*figure S2b*).

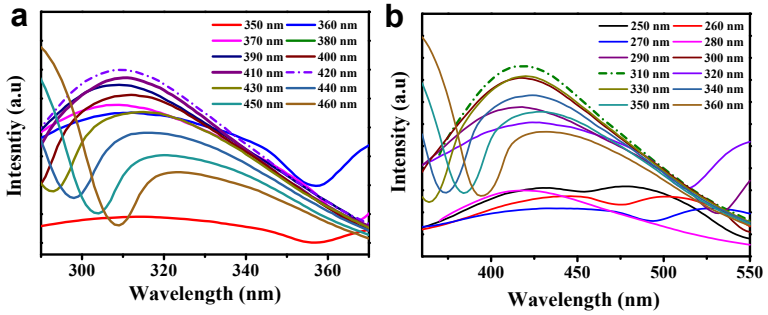

Figure S2. (a) Emission Spectra & (b) Excitation spectra of Ph-SF composite

Figure S3(a) shows the change in PL intensity of probe and probe + analyte with respect to temperature. We have carried out the analysis in the temperature range of 15- 50 °C. First, we have prepared the probe and probe + analyte solution. For the probe, we took 500 µL Ph-SF, 2 mL water, and 200 µL PBS and mixed all of them properly. Similarly, for probe + analyte, into the probe solution (500 µL Ph-SF + 2 mL water + 200 µL PBS) we have added 10 µL of Chol and carried out the analysis. We have analyzed the change in PL intensity with respect to time as shown in the figure below. It has been observed that with an increase in the temperature, the PL intensity

decreases. *Figure S3(b)* shows the bar diagram that represents the change in pH. To find out the optimum pH, where the fluorescent intensity is maximum we have checked the effect of pH in the case of probe and probe + analyte at different pH levels in the range 3-12. It has been observed in both cases that with an increase in the pH, there is a gradual increase in the PL intensity. At pH~ 7 it shows a maximum intensity. After further increase in the pH, the PL intensity again tends to decrease.

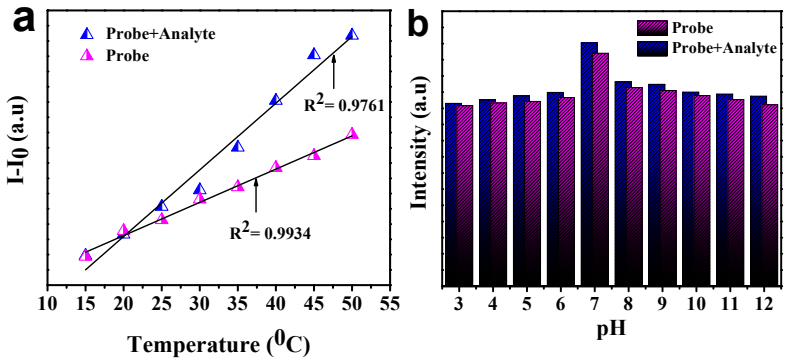

Figure S3. (a) Temperature dependency of Ph-SF and Ph-SF + Cholesterol & (b) pH dependency of Ph-SF and Ph-SF + Cholesterol

Figure S4 shows the UV-Vis spectra of the probe with different amounts of analyte i.e., Chol. It has been observed from the graph that there is no such change was observed even after the addition of the Chol. Apart from this, no new peak appeared which means that no ground state complexation is taking place. This means that the fluorescence is not static in nature, it may be dynamic.

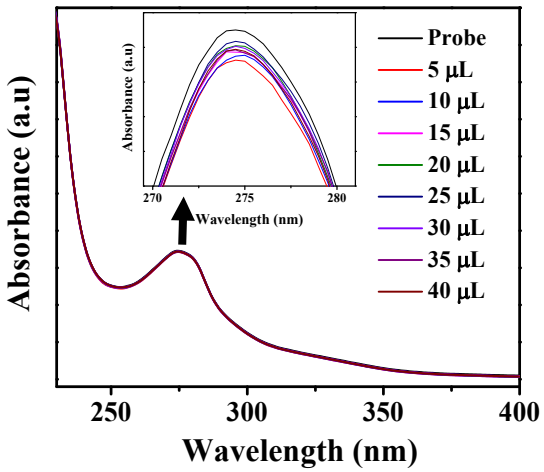

Figure S4. UV-visible spectra of the probe with different Chol volumes.

To get more insight into the mechanism and to differentiate between the dynamic and static nature of the probe, we have done the time-resolved photoluminescence (TRPL) study. We have analyzed how the lifetime changes after the addition of the analyte. The determined lifetime (χ^2) value for probe and probe + analyte was about 7.43 ns and 7.39 ns respectively. This means that even after the addition of the analyte the lifetime of the probe does not change significantly which is evident from *Figure S5*. This finding favours the fact that the change in fluorescence intensity is dynamic in nature.

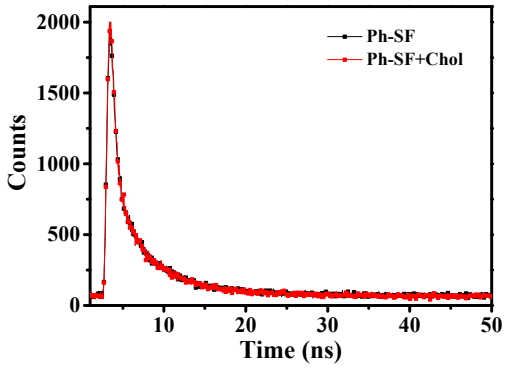

Figure S5. TRPL spectra of Ph + SF and Ph + SF + Chol

Figure S6 represents the overlap spectra of the absorbance spectra of the analyte with the emission and excitation spectra of the probe i.e., Ph-SF. It is evident from the following figure that the overlap is mainly taking place between the absorbance of the analyte and the excitation spectra of the probe. This fulfills the criteria for having an IFE mechanism. The schematic representation of the interaction of Chol with Ph + SF is in *scheme S1*.

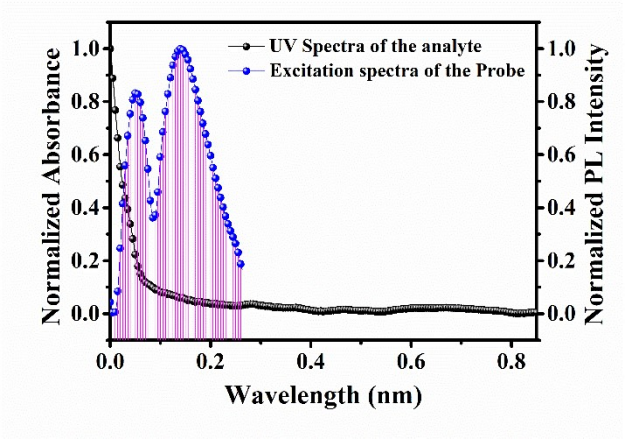

Figure S6. Overlap spectra of absorbance spectra of the analyte with the emission as well as excitation spectra of the probe

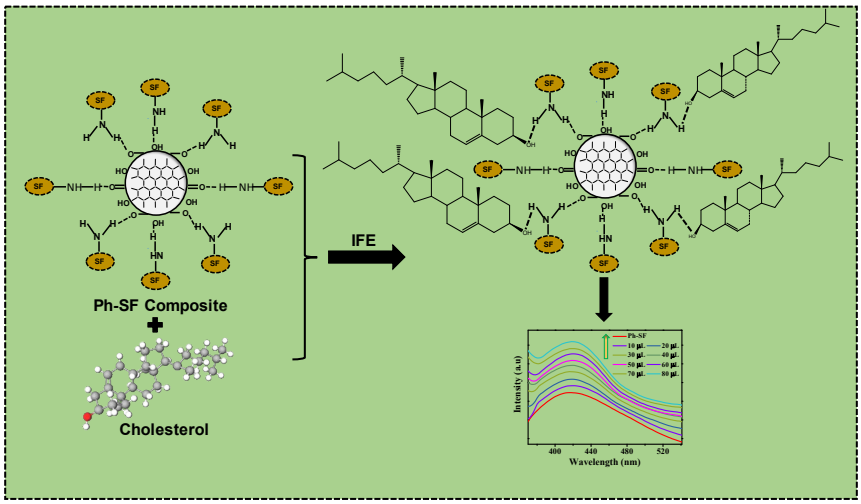

Scheme S1. The schematic representation of the interaction of Chol with Ph + SF via the IFE mechanism

Figure S7 represents the zeta potential distribution graph of Ph, Ph-SF, Chol, and Ph-SF + Chol. After the addition of Chol the increase in the fluorescent intensity of Ph-SF can be confirmed further with the help of electrostatic interaction and H- bonding. The electrostatic interaction between the probe and the analyte has to be in close proximity. To confirm that we have recorded the zeta potential (ζ) value. The ζ value for Ph, Ph SF, Chol, and Ph-SF + Chol was found to be about -22.9 mV, -16.4 mV, -7.54 mV, and -12.7 mV respectively. This indicates the accumulation of charge as considerable change was observed in the zeta potential value after interacting with Chol. This confirms that the interaction between the probe and the analyte is electrostatic.

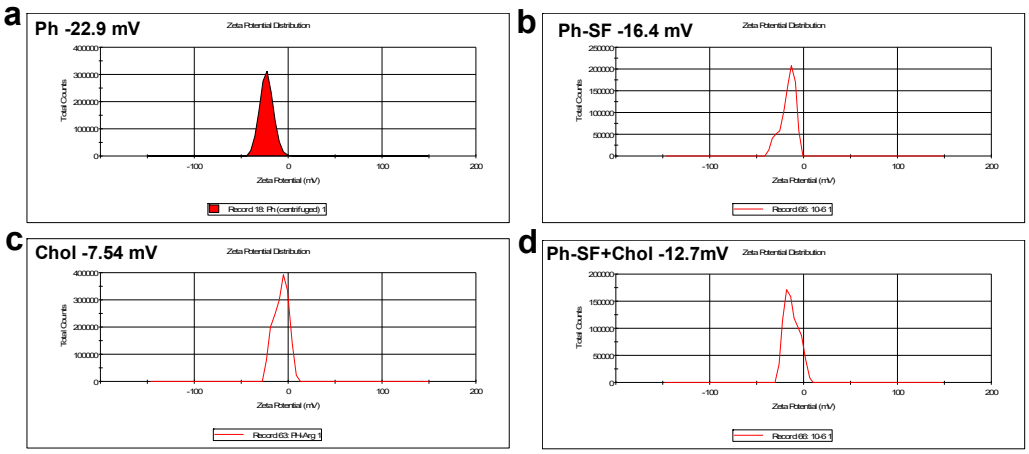

Figure S7. Zeta potential distribution graph of (a) Ph; (b) Ph-SF; (c) Chol; and (d) Ph-SF + Chol

Figure S8 shows the FTIR spectra of Ph-SF and Ph-SF + Chol. The IFE and electrostatic interaction can also be interpreted by taking the reference of H-bonding. Chol has one –OH group present in it, which can form an H-bonding with the Ph-SF composite. We have also analyzed the FTIR spectra of the Ph-SF before and after the addition of the analyte. It has been observed that the FTIR spectra do not involve much change after the addition of Chol. However, the intensity of a few peaks was reduced and a few of that got shifted. This confirms the formation of H- bonding between the probe and the analyte.

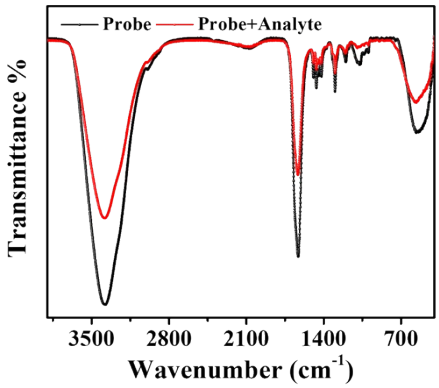

Figure S8. FTIR spectra of Ph-SF and Ph-SF + Chol

Figure S9 shows the intensity graph and the bar diagram of the same. We have selected biomolecules such as fructose, glycine, alanine, ascorbic acid, cysteine, folic acid, urea, thiamine, aspartic acid, proline, vitamin B12,

and ions like Fe^{3+}, K^{+}, Na^{+}, Cu^{2+}, Mg^{2+}, Ca^{2+}. It has been observed from the analysis that the material is highly selective for Chol irrespective of any other interfering agents.

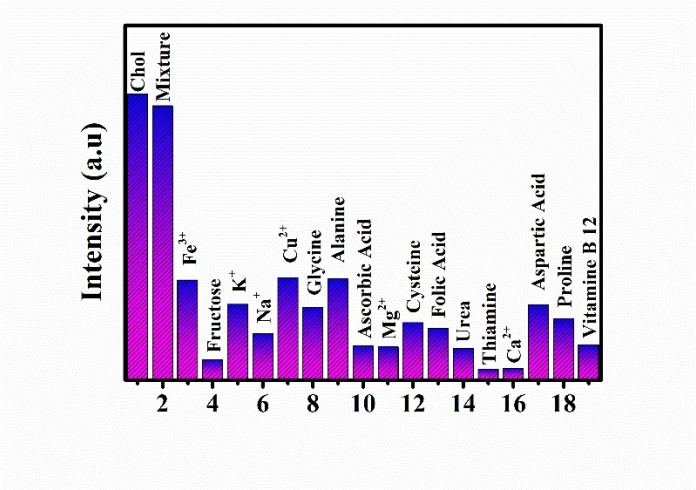

Figure S9. Bar diagram for the interference study of Ph-SF with different biomolecules and ions

After successful coating of the CNM with Ph-SF we have recorded the FE-SEM images of CNM and CNM+Ph-SF. *Figure S10(a & b)* shows the SEM images of CNM in the scale 2 µm and 1 µm respectively. This image signifies that the membranes are microporous in nature. Due to its microporous nature, it can uptake material effectively. To confirm the uptake efficiency, we have taken the SEM images after the coating with Ph-SF as shown in *Figure S10(c & d).* From the figure it has been observed that the pores initially present on the surface were reduced. This signifies the occupancy of the pores present in the CNM by Ph-SF.

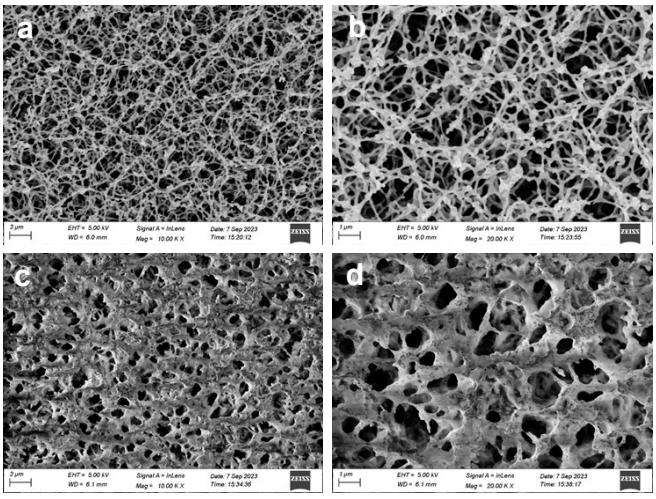

Figure S10. FESEM images of (a & b) CNM and (c & d) CNM+Ph-SF

The stability of an ideal sensor is one of the prime concerns of a fabricated sensor. To analyze that we have checked its I-V characteristics at different humid conditions as shown in *Figure S11*. Cu adhesives have been attached to both the ends of the strips 0.4 mm apart which will act as electrodes. We have recorded the I-V

characteristics of the prototype devices in humid conditions like 30, 40, 50, 60, and 70 % (RH). This signifies that the sensor is stable under different humid conditions.

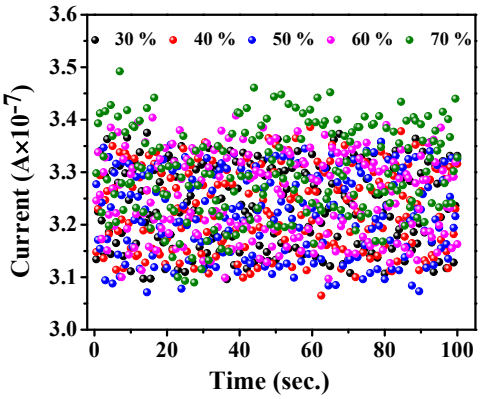

Figure S11. I-V characteristic of the fabricated device under different humid conditions ranging from 30- 70 % (RH)

Figure S12 shows the I-V characteristic of the strips i.e., CNM and CNM + Ph-SF in the absence and presence of Chol. For CNM, CNM + Ph-SF, and CNM + Ph-SF + Chol the current values were found to be about 5.46×10^{-9} A, 7.74×10^{-6} A, and 2.16×10^{-5} A respectively. It is prominent from the values as well as the graph that the fabricated device can effectively detect Chol as shown in *Figure S12(a)*. We have also optimized the concentration of the Ph-SF as shown in *Figure S12 (b)*. It has been observed that with an increase in the concentration of the Ph-SF, the current value increases up to 8×10^{-6} A. Similarly, we have also varied the concentration of the Chol in the linear range of 1-5 mM as shown in *Figure S12(c)*. In this case, also it has been observed that the current value increases with an increase in the Chol concentration. *Figure S12(d)* shows the calibration graph for aqueous media. We have calculated the LOD through calibration graph which was found to be about 0.263 µM.

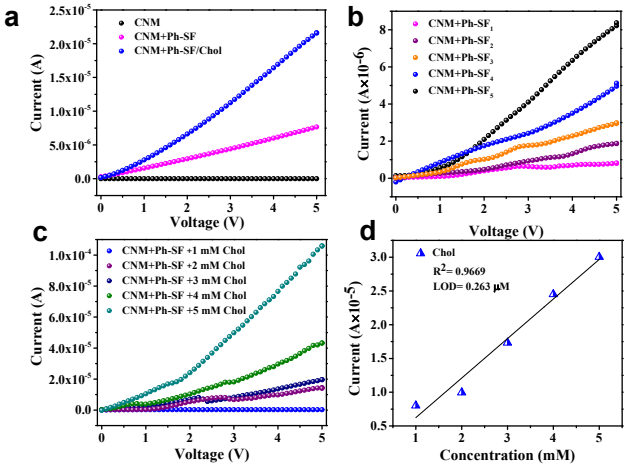

Figure S12. (a) Comparison of I-V characteristics of CNM, CNM + Ph-SF, and CNM + Ph-SF + Chol; (b) Optimization of the device with different concentrations of Ph-SF; (c) Comparison of I-V characteristics with different concentrations of Chol; (d) Calibration graph

Transport number is one of the analytical parameters with the help of which one can determine whether a material is electrically conductive or ionically conductive. This approach is based on the Wagner polarisation technique. In this method, to induce ionic or electronic conductivity, a voltage is given to the prototype device. If the material shows a current that is constant with respect to time, then the material is said to be electrically conductive. In contrast, if the current value gradually decreases with an increase in time to a certain point where it reaches a steady state after which it shows constant current with time then it is said to be ionically conductive. In this case, also we have checked the pattern of transport in the presence as well as the absence of Chol as shown in *Figure S13*. For the analysis, we connected the end of the prototype devices into crocodile clips and applied a voltage of about 0.1 V to observe the change in current-voltage (I-V) change. The change in transport number before and after the addition of Chol is in the supplementary file *Figure S13*. Before interacting with Chol the blank device shows constant current with respect to time. This means that the device is electronically conducting. However, upon interacting with Chol, under the influence of the step voltage, the ionic movement takes place until it attains a steady state. After reaching the steady state, the device got polarized and showed constant current with respect to time.

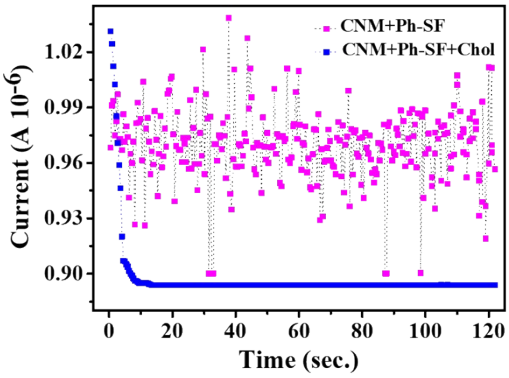

Figure S13. Transport number analysis of CNM+Ph-SF and CNM+Ph-SF+Chol

After that, we analyzed the FTIR spectra of the devices before and after came in contact with Chol as shown in *Figure S14.* As observed from the figure, there is no significant change observed. However, few of the peaks shifted towards the lower wavelength as shown in *Table S1*. This can be confirmed by the fact that, as cholesterol has only one –OH group present, it can readily form an H-bond with the free functional groups present in the Ph-SF composite.

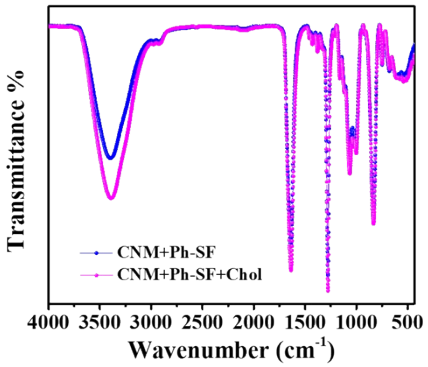

Figure S14. FTIR spectra of CNM+Ph-SF before and after coming in contact with Chol.

Table S1- Change in FTIR frequencies after coming in contact with Chol

CNM+Ph-SF	**3391**	**1637**	**1456**	**1427**	**1377**	**1276**	**1160**	**1063**	**1023**	**1000**	**833**	**748**	**675**	**538**
CNM+Ph-SF+Chol	3384	1634	1454	1427	1376	1275	1159	1063	1023	998	832	748	673	537

The bar diagram that represents the interference study of the material with different biomolecules and ions is shown in *Figure S15*. To check the efficacy of the fabricated device we have taken some biomolecules and ions into consideration. For biomolecules, we have chosen urea, alanine, thionine, ascorbic acid, aspartic acid, proline, vitamin B12, cysteine, folic acid, glycine, fructose, dopamine, biotin, glutamic acid, oxalic acid, valine, serine, lysine, and threonine. For ions we have chosen Na^{+}, Mg^{2+}, Cu^{2+}, Ca^{2+}, Fe^{3+}, K^{+}, and Zn^{2+}. It has been observed from the graph that the material is highly selective for the detection of Chol even in the presence of other biomolecules and ions.

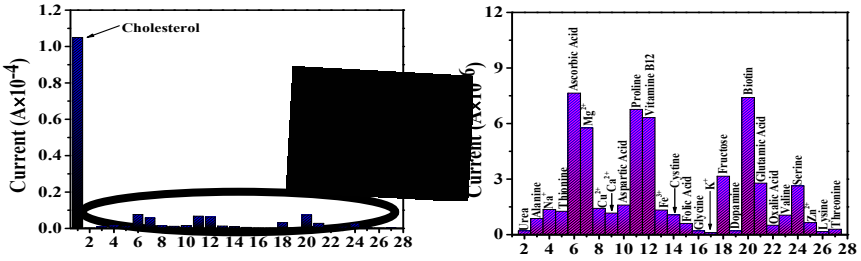

Figure S15. Interference of the fabricated CNM+Ph-SF with different biomolecules and ions apart from Chol.